Journal of Statistical Physics, Vol. 101, Nos. 1/2, 2000

Recent Theoretical Developments on the Formation of Liesegang Patterns[1]

Michel Droz[2]

Received November 15, 1999; final March 15, 2000

When an electrolyte A diffuses into a gel containing another electrolyte B, the eventual formation of a rhythmic pattern of precipitate by the moving chemical reaction front is known as the *Liesegang phenomenon*. Although the Liesegang phenomenon has been studied for a century, the mechanisms responsible for these structures are still under discussion. However, recently, important theoretical progresses have been made towards a theoretical understanding of this phenomena. A critical analysis of the present state of the art as well as a discussion of some open problems is presented.

KEY WORDS: Pattern formation; Liesegang patterns; reaction-diffusion; spinodal decomposition; kinetic Ising model; competing dynamics.

1. INTRODUCTION

A typical experiment exhibiting Liesegang pattern formation consists of a test tube containing a gel in which a chemical species B (for example $AgNO_3$ or $MgCl_2$) is uniformly distributed with concentration b_0. Another species A, with concentration a_0 (for example HCl or NaOH) is allowed to diffuse into the tube from its open extremity and chemically react with B. As this reaction goes on, formation of consecutive bands of precipitate (AgCl or $Mg(OH)_2$ in our example) is observed in the tube, provided that the concentration a_0 is large enough compared to b_0 so that the reaction propagates along the tube[1–3] (see Fig. 1).

A striking feature of this process is that, after a transient time, these bands appear at some positions x_n and times t_n that obey simple generic laws.

[1] Invited talk given at the *Nonlinear Science: Dynamics and Stochasticity*, NATO advanced workshop hold in Brussels, June 30–July 3 (1999).

[2] Department of Theoretical Physics, University of Geneva, CH-1211 Genève 4, Switzerland.

0022-4715/00/1000-0509$18.00/0

Fig. 1. Typical example of Liesegang patterns obtained with the reagents $A = \mathrm{NaOH}$ and $B = \mathrm{MgCl_2}$ in a gel. The light grey precipitate is $D = \mathrm{Mg(OH)_2}$. The experiments were carried out by M. Zrínyi (Technical University of Budapest).

First, the position of the nth band x_n is proportional to $\sqrt{t_n}$ where t_n is the time elapsed until the appearance of the band. This is the so-called *time law*.[4] Secondly, the positions x_n usually form a geometric series (*spacing law*):[5]

$$x_n \to Q(1+p)^n \tag{1.1}$$

for n large. $p > 0$ is called the spacing coefficient and Q is the amplitude of the spacing law. Finally, the width w_n of the bands have been observed to increase with n and to obey the *width law*, $w_n \sim x_n^{\alpha}$, where the exponent α is close to 1.[6] Most of the detailed experimental observations concern the spacing law. It turns out that the spacing coefficient p is a nonuniversal quantity depending on the experimentally controllable concentrations a_0 and b_0 of the outer (A) and inner (B) electrolytes. This dependence is expressed by the *Matalon–Packter law*:[7, 8]

$$p = F(b_0) + G(b_0)\frac{b_0}{a_0} \tag{1.2}$$

where F and G are decreasing functions of their argument.

The presence of bands is related to the geometry of the experiment, i.e., the use of a test tube with axial symmetry and most of the experiments have been performed in such a system. However, for more complicated geometries, different shapes may be obtained. A well known example is provided by the rings formed in agate rocks.[1, 2, 5]

2. THEORIES WITH THRESHOLDS

The time law turns out to be a simple consequence of the diffusion process. It is well known that the reaction front position $x_f(t)$ obeys the relation $x_f(t) \sim \sqrt{t}$, with an amplitude depending on the the concentrations a_0 and b_0 and the diffusion coefficients D_a and D_b. However, the explanation of the spacing and width laws are not so simple. Several theoretical models of the Liesegang phenomena have been recently studied and simple expressions for the spacing coefficients characterizing the patterns

were derived.[9] The emphasis was on displaying the dependences on the concentrations of the inner- and outer-electrolytes. Competing theories (ion-product supersaturation, nucleation and droplet growth, induced sol-coagulation) were treated with the aim of finding the distinguishing features of the theories. All these theories follow how the diffusive reagents A and B turn into immobile precipitate D

$$A + B \rightarrow \cdots C \cdots \rightarrow D \tag{2.1}$$

by taking into account various scenarios for the intermediate steps denoted as $\cdots C \cdots$. Since the precipitate appears through some kind of supersaturation, further differences in theories arise from the details of treating the nucleation thresholds and the growth kinetics of the precipitate.

The simplest (and first developed) theory is based on the concept of *supersaturation of ion-product*[10] and has been developed by many researchers.[11–15] In this theory, there is no intermediate step between A, B and D. When the local product of the reactants concentrations, ab, reaches some critical value q^* nucleation of the precipitate D occurs. The nucleated particles grow and deplete the A and B populations in their surroundings. As a consequence, the local level of ab drops and no new nucleation takes place. This continues until the reaction zone (where ab is maximum) moves far enough that the depletion effect of the precipitate becomes weak. The local concentration b which droped to zero when the band was formed is increasing again and, eventually, the condition $ab = q^*$ is fulfilled again and nucleation can occur. This mechanims is decribed in details and illustrated with a picture in ref. 9. The repetition of this process leads to the formation of bands.

In the next level of complexity, theories contain a single intermediate step in $\cdots C \cdots$ with the mechanism of band formation based on the supersaturation of the intermediate compound C.[16, 17] It is assumed that A and B react to produce a new species C which also diffuses in the gel. C may be a molecule or a colloid particle. When the local concentration of C reaches some threshold value c^n, nucleation occurs and the nucleated particles, D, act as aggregation seeds. The C particles near to D aggregate to the existing droplet (hence become D) provided their local concentration is larger than a given aggregation threshold c^a. These models are characterized by two thresholds, one for nucleation and one for droplet growth. The depletion mechanism is similar to the one described for the ion-product theory and it leads to band formation. These are the basic mechanisms of the so-called theory of *nucleation and droplet growth*. A variation of the single intermediate compound theories is based on the idea of an *induced sol-coagulation* process[18]). The compound C is assumed

to be the sol and this sol coagulates if the following two conditions are satisfied: first, the concentration of C exceeds a supersaturation threshold $c \geqslant c^n$ and, second, the local concentration of the outer electrolyte is above a critical coagulation concentration threshold $a > a^*$. The band formation is a consequence of the nucleation and growth of the precipitate combined with the motion of the front where $a = a^*$. The comparison of the predictions given by the above theories for the time- and the spacing laws with the Matalon–Packter law allowed us to select the best theory. The analytical computation of the spacing parameters was possible only under some simplifying assumptions.[9] The simple emerging picture allowed us to conclude that, among the theories described above, the ones with an intermediate species C were the best in describing the experimental observations. However, the drawbacks of all the above models are that they contain threshold parameters such as e.g., q^*, c^n, c^a, a^* that are difficult to control experimentally and not easy to grasp theoretically. Accordingly, we recently proposed a new scenario, free of arbitrary thresholds.[19]

3. THE SPINODAL DECOMPOSITION SCENARIO

In the experiments, once the Liesegang patterns are formed they are frozen, i.e., they do not evolve anymore on any reasonable observation times (up to several years). This fact suggests that a phase separation mechanism takes place in the formation of bands. Moreover, this process should take place at a very low effective temperature, as no coarsening of the bands is experimentally observed. The dynamics of phase separation is a well understood problem.[20, 21] When one quenches a system having a phase transition below the coexistence curve, the system separates in two phases. Two cases have to be distinguished. When the quench takes place near the coexistence curve, the system finds itself in a metastable state. Small droplets of the minority phase are formed and grow with time. This is a slow process due to the presence of an activation energy. This process is called homogeneous nucleation. On the other hand, when one quenches the system far from the coexistence curve, the systems finds itself in an unstable state. No activation energy is involved and the phase separation starts immediately; this process is called spinodal decomposition. The two regimes (nucleation and spinodal decomposition) are separated by the so-called spinodal line. Note that this line is a mean-field like concept and in real systems, there is a smooth crossover from one regime to the other.

According to the discussion given in Section 2, we restrict ourselves to the intermediate-compound theories for the formation of Liesegang patterns. The problem is then to imagine how a phase separation could occur in such a system, and we recently have proposed a simple mechanism to

achieve this goal.[19] As a result of the $A + B \to C$ reaction-diffusion process, a moving reaction-diffusion front is present. This front puts down locally some C particles. Once deposited, the C particles diffuse. Small clusters of particles nucleate at and aggregate behind the front. However, the nucleation is an activated process and its characteristic time-scale τ_{nucl} is large at low temperatures. If τ_{nucl} is much larger than the time τ_{front} needed by the front to put out the local concentration c_0 then the system reaches the unstable state, i.e., crosses the spinodal line.[20] Once the spinodal line is crossed, the phase separation takes place on a short time-scale and a domain formed by C particles is rapidly formed at or behind the front, hence the formation of a Liesegang band.

This band acts as a sink for the particles and, in the vicinity of the band, the local concentration of particles decreases and the front is no longer in the unstable region of the phase space. When the front moves far enough, the depleting effect of the band diminishes. Thus the concentration of particles grows and the spinodal line is crossed again resulting in the formation of the next band. The repetition of this process should lead then to the Liesegang pattern. In this scenario, the properties of the reaction-diffusion front ($A + B \to C$) is a essential ingredient. These have been studied in great details by Gálfi and Rácz.[22] The center of the front moves as $x_f(t) = \sqrt{2D_f t}$, where the diffusion constant D_f is given by $\text{erf}(\sqrt{D_f/2D}) = (a_0 - b_0)/(a_0 + b_0)$ with $D = D_a = D_b$ being the diffusion coefficient of the A and B particles. Moreover, the width of the front increases with time as $w(t) = 2\sqrt{D}\, t^{1/6}/(ka_0K)^{1/3}$ where k is the reaction rate of the $A + B \to C$ process, and $K = (1 + b_0/a_0)(2\sqrt{\pi})^{-1} \exp(-D_f/D)$. Note that these predictions result from a mean-field approximation which has been shown to be valid in dimensions $d \geqslant 2$.[23]

A more familiar description of a spatially discretized version of the problem can be formulated in terms of a spin-1/2 kinetic Ising system. Empty and occupied lattice sites are associated with down and up spins, respectively. The initial state is empty (all spins are down) and the moving front flips the down spins at a given rate. This process can be described by Glauber dynamics,[24] while the diffusion is described by a spin exchange process or Kawasaki dynamics.[25] The rates of exchanges entering into the Glauber and Kawasaki dynamics are governed by a heat bath at temperature T. Moreover, one assumes ferromagnetic couplings between the spins to model the attraction among the C particles. Thus we end up with a kinetic Ising model with competing dynamics at very low temperature, for the reasons explained above. The local magnetization m and particle density c are simply related by $m = 2c - 1$.

Let us now consider qualitatively how bands can emerge in this model. One starts from a state with all the spins down (S_I in Fig. 2). As explained

in details in ref. 22, the reaction front leaves behind a constant density c_0 of C particles, thus correspondingly the spin-flipping front produces a local magnetization $m_0 = 2c_0 - 1$. As we would like the front to bring the system into the unstable state, we assume that $m_0 > -m_s$. As time evolves, the local state moves from S_I towards S_0 (Fig. 2). The system crosses successively the coexistence line ($m = -m_e$) and the spinodal line ($m = -m_s$) and ends up into the unstable states domain where phase separation takes place. Thus a spin-up domain (i.e., a band) is rapidly formed at or behind the front. This mechanism is possible because at low temperature, the time scale for nucleation is much larger than the time needed by the front to put the system in the unstable states domain. The new band acts as a sink for the up-spins being in its vicinity. Thus, the local magnetization decreases and the front is no longer in the unstable domain. However, when the front has moved far enough, the depleting effect of the band disappears. The front can bring again the system into the unstable domain and a new band is formed. In summary, the new feature of this scenario is the assumption that the state of the front is quasiperiodically driven into the unstable states domain. Before investigating the properties of this model at a microscopic

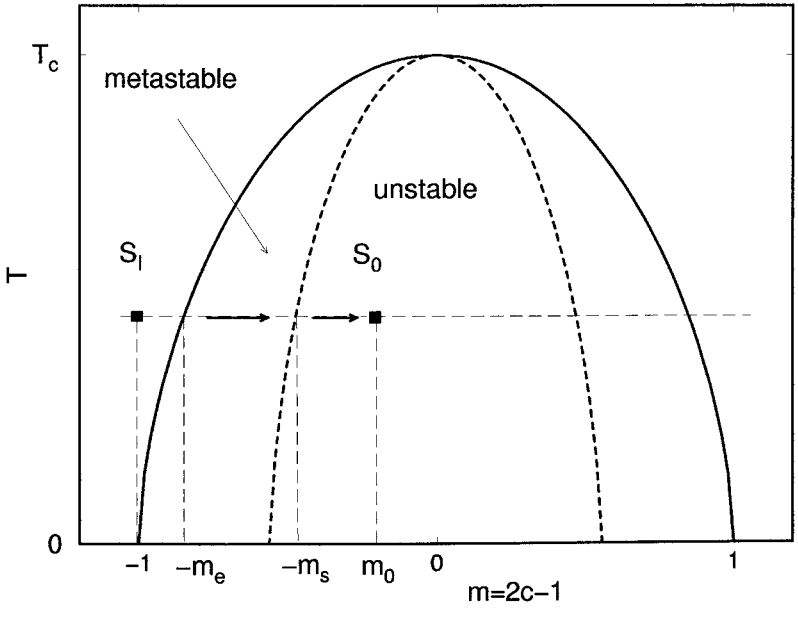

Fig. 2. Qualitative phase diagram for the Ising model. The solid line is the coexistence curve and the dashed one is the spinodal line. S_I is the initial state with $m = -1$, $\pm m_e$ are the equilibrium magnetizations at a given temperature T while $\pm m_s$ are the magnetizations at the spinodal line.

level, one can first study a mesoscopic version of it. At a coarse grained level, the diffusive dynamics of the magnetization m is described by Model B of critical dynamics.[26] The Glauber dynamics part is modeled by adding a time-dependent source term S. Thus the equation of evolution for the local magnetization is:

$$\partial_t m = -\lambda \Delta(\varepsilon m - \gamma m^3 + \sigma \Delta m) + S \tag{3.1}$$

Here λ is a kinetic coefficient, ε measures the deviation from the critical temperature T_c and $\varepsilon > 0$ ensures that $T < T_c$. The parameter γ is positive to guarantee overall stability and $\sigma > 0$ provides the stability against short-wavelength fluctuations.

Having in mind to explain the experimental patterns obtained in long test tubes, (axial symmetry) we assume that m and S depend only on a single spatial coordinate, thus $m = m(x, t)$ and $S = S(x, t)$.

In first approximation we neglect both the thermal noise and the fluctuations in the reaction diffusion front. We shall return to the problem of the fluctuations in the following section. The source term S can be described to an excellent accuracy[27] by the following gaussian form:

$$S(x, t) = \frac{\mathscr{A}}{t^{2/3}} \exp\left[-\frac{[x - x_f(t)]^2}{2w^2(t)} \right] \tag{3.2}$$

with

$$\mathscr{A} = 0.3 k a_0^2 K^{4/3} \tag{3.3}$$

Equation (3.1) can be solved numerically using the initial condition $m(x, t) = -m_h$ the globally stable solution in the absence of a source term ($S = 0$), and starting the source at the origin. The solution depends crucially on the value of m_0.

If m_0 is such that the system is deep inside the unstable domain, well defined Liesegang bands form from the very beginning, as seen on Fig. 3. However, if m_0 is near the spinodal value then, at early stages of the evolution, a nearly periodic set of narrow bands emerges that coarsens with time. Later on, the newly formed pattern crosses over to Liesegang-type patterns.

Once formed, the Liesegang-type bands are static on the time-scale we are able to observe. Their spacing is well defined and the data for x_n are very well fitted by a two-parameter function of the form $x_n = Q[\exp(\tilde{p}n) - 1]$ as shown in Fig. 4. Thus the spacing law is reproduced with $1 + p = \exp(\tilde{p})$.

The dependence of p on the concentrations a_0 and b_0 was also investigated and we found a good agreement with the linear dependence in

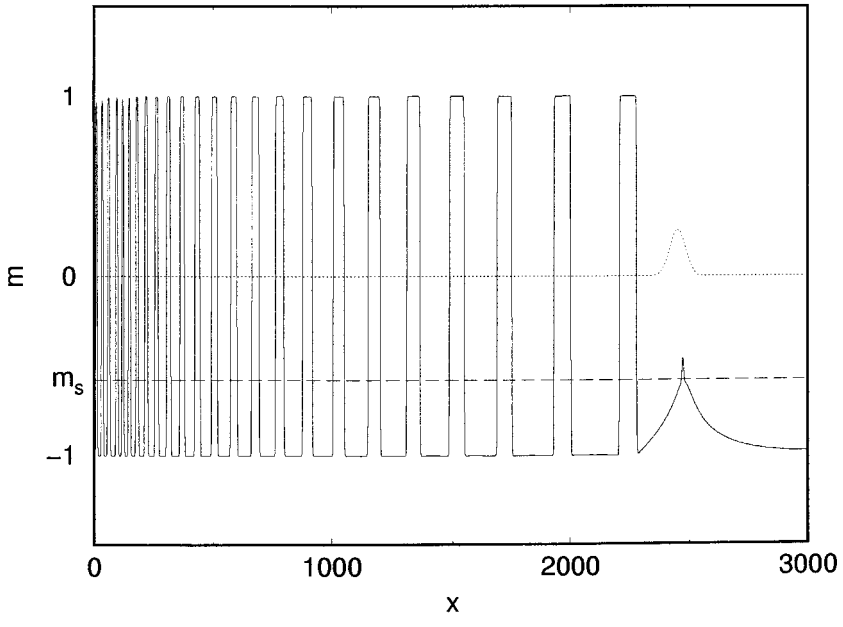

Fig. 3. Magnetization profile obtained for the values of parameters: $D_f = 21.72$, $w_0 = 4.54$, and $\mathscr{A} = 0.181$. The length, time, and the magnetization are measured in units of $\sqrt{\sigma\varepsilon}$, $\sigma/(\lambda\varepsilon^2)$, and $\sqrt{\varepsilon/\gamma}$, respectively. The dotted line denotes the rate of local magnetization increase due to the source, S, measured in units of $\lambda\varepsilon^{5/2}/(\gamma^{1/2}\sigma)$ and magnified by a factor $2 \cdot 10^5$. The dashed line is the magnetization at the spinodal line, $m_s = -1/\sqrt{3}$.

b_0/a_0 as predicted by the Matalon–Packter law.[19] Moreover, a power-law fit form gave $F(b_0) \sim b_0^{-1.7}$ and $G(b_0) \sim b_0^{-1.1}$, confirming the decreasing character of these functions. Finally, the dependence of the amplitude Q on the spacing law on the concentrations a_0 and b_0 was found to be of the form $Q(a_0, b_0) \sim (a_0/b_0)^{0.4}$. Such prediction can have important consequences when analyzing the experimental data.

The problem of the relevance of this model in explaining the experimental data remains to be discussed. Using realistic values for the different parameters entering into the theory, one can predict the time and space scales on which the patterns shows up. This issue has been recently carefully discussed by Rácz.[28] It was shown that indeed the theoretical predictions are compatible with the experimental findings.

4. THE ROLE OF THE FLUCTUATIONS

Most of the theoretical models discussed in the literature do not take the fluctuations into account. The only exception is the nucleation and

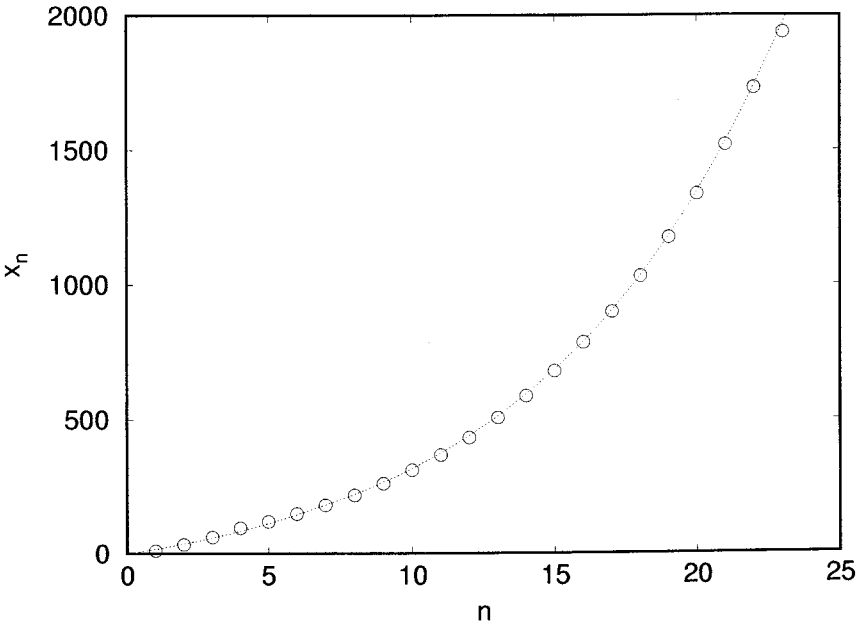

Fig. 4. Positions of the bands x_n vs their order of appearance n. Length is measured in units of $\sqrt{\sigma\varepsilon}$. The full line is hte best fit of the form $x_n = Q[\exp(\tilde{p}n) - 1]$.

growth model investigated by Chopard *et al.*[17] This cellular automata approach to the formation of Liesegang patterns was able to reproduce many experimentally observed aspects. In particular, the fact that fluctuations were properly treated lead, in two dimensions, to patterns with broken symmetry (spirals instead of rings). Such spiral patterns as well as helix in test-tubes are experimentally observed[29] and obviously they cannot be obtained from an analytical theory based on deterministic equations with cylindrical symmetry.

Our simple spinodal decomposition scenario is offering us new ways to investigate the role of the noise in these systems. Two directions can be investigated. First, at the mesocscopic level, one can add a noise term to the equation of motion (3.1). The problem is to find the appropriate noise modeling both the thermal and reaction-diffusion fluctuations. Second, one can carry out Monte-Carlo simulations of the kinetic Ising model with competing dynamics described above. The problem is there to find the good window in the parameters space in which spinodal decomposition occurs. It is experimentally well known that Liesegang patterns are only formed for a rather restricted range of parameters. Work along these lines is in progress.[30]

5. CONCLUSIONS

In conclusion we have proposed a new scenario for the formation of Liesegang patterns, based on a spinodal decomposition mechanism. Our approach has the advantage of involving only a small number of parameters and eliminating the need to introduce artificial thresholds. Our model yields the Matalon–Packter law and allows the calculation of both the spacing coefficient $p(a_0, b_0)$ and the amplitude $Q(a_0, b_0)$ of the spacing law.

However, one has to recognize that the above scenario cannot explain all the experimental observations and conditions related to the formation of Liesegang patterns. For example, band formation during gaseous diffusion in aerogels has recently been observed.[31] Also for the usual case of reaction-diffusion in a gel described above, one sometimes observes the phenomenon of reverse banding in which the spacing between consecutive bands decreases. None of these two cases are today evidently compatible with the spinodal decomposition scenario.

Thus, several challenging problems remain open in this fascinating field of pattern formation in nonequilibrium systems to which Prof. Grégoire Nicolis made several important contributions.

ACKNOWLEDGMENTS

I thank T. Antal, B. Chopard, J. Magnin, A. Pekalski, Z. Rácz and M. Zrinyi, for useful discussions on this topic. This work has been partially supported by the Swiss National Science Foundation.

REFERENCES

1. R. E. Liesegang, *Naturwiss. Wochenschr.* **11**:353 (1896).
2. R. E. Liesegang, *Photog. Archiv.* **21**:221 (1896).
3. H. K. Henisch, *Periodic Precipitation* (Pergamon Press, 1991).
4. H. W. Morse and G. W. Pierce, *Proc. American Academy of Arts and Sciences* **38**:625–647 (1903).
5. K. Jablczynski, *Bull. Soc. Chim. France* **33**:1592 (1923).
6. M. Droz, J. Magnin, and M. Zrínyi, *J. Chem. Phys.* **110**:9618 (1999).
7. R. Matalon and A. Packter, *J. Colloid Sci.* **10**:46 (1955).
8. A. Packter, *Kolloid Zeitschrift* **142**:109 (1955).
9. T. Antal, M. Droz, J. Magnin, Z. Rácz, and M. Zrinyi, *J. Chem. Phys.* **109**:9479, (1998).
10. W. Ostwald, *Lehrbuch der Allgemeinen Chemie* (Engelman edt., Leipzig, 1897).
11. C. Wagner, *J. Colloid Sci.* **5**:85 (1950).
12. S. Prager, *J. Chem. Phys.* **25**:279 (1956).
13. Ya. B. Zeldovitch, G. I. Barrenblatt, and R. L. Salganik, *Sov. Phys. Dokl.* **6**:869 (1962).
14. D. A. Smith, *J. Phys. Chem.* **81**:3102 (1984).
15. G. Venzl and J. R. Ross, *J. Chem. Phys.* **77**:1302 (1982); S. C. Müller, S. Kal, and J. R. Ross, *J. Phys. Chem.* **86**:4078 (1982); M. E. LeVan and J. R. Ross, *J. Phys. Chem.* **91**:6300 (1987).

16. G. T. Dee, *Phys. Rev. Lett.* **57**:275 (1986).
17. B. Chopard, P. Luthi and M. Droz, *Phys. Rev. Lett.* **72**:1384 (1994); *J. Stat. Phys.* **76** (1994).
18. S. Shinohara, *J. Phys. Soc. Japan* **29**:1073 (1970).
19. T. Antal, M. Droz, J. Magnin, and Z. Rácz, *Phys. Rev. Lett.* **83**:2880 (1999).
20. J. D. Gunton, M. San Miguel, and P. S. Sahni, The dynamics of first order transitions, in *Phase Transition and Critical Phenomena*, Vol. 8, C. Domb and J. L. Lebowitz, eds. (Academic Press, 1983).
21. J. D. Gunton and M. Droz, *Introduction to the Theory of Metastable and Unstable States*, Lecture Notes in Physics, Vol. 183 (Springer-Verlag, 1983).
22. L. Gálfi and Z. Rácz, *Phys. Rev. A* **38**:3151 (1988).
23. S. Cornell and M. Droz, *Phys. Rev. Lett.* **70**:3824 (1993)
24. R. J. Glauber, *J. Math. Phys.* **4**:294 (1963).
25. K. Kawasaki, *Phys. Rev.* **145**:224 (1966).
26. P. C. Hohenberg and B. I. Halperin, *Rev. Mod. Phys.* **49**:435 (1977).
27. H. Larralde, M. Araujo, S. Havlin, and H. E. Stanley, *Phys. Rev. A* **46**:855 (1992).
28. Z. Rácz in the proceedings of the NATO Advanced Workshop on *Statistical Physics Applied to Practical Problems* (Budapest, 1999), to be published.
29. J. S. Kirkaldy, *Rep. Prog. Phys.* **55**:723 (1992).
30. T. Antal, M. Droz, J. Magnin, A. Pekalski, and Z. Rácz (to appear).
31. M. A. Einarsrud, F. A. Maao, A. Hansen, M. Kiekedelen, and J. Samseth, *Phys. Rev. E* **57**:6767 (1998).